



Dual-wavelength dispersion-managed soliton all-fiber mode-locked laser based on birefringence-filtered nonlinear polarization evolution

Shuang Niu¹, Runmin Liu¹, Defeng Zou, Youjian Song^{*}, Minglie Hu^{*}

Ultrafast Laser Laboratory, Key Laboratory of Opto-electronic Information Science and Technology of Ministry of Education, School of Precision Instruments and Optoelectronics Engineering, Tianjin University, 300072 Tianjin, China

ARTICLE INFO

Keywords:

Nonlinear polarization evolution
Dispersion-managed
Dual-wavelength mode-locking

ABSTRACT

Single-cavity dual-comb mode-locked lasers, an emerging dual-comb technology, can generate two sets of pulse sequences with excellent mutual coherence, thus eliminating the need for complex active noise reduction systems. We report the generation of dual-wavelength dispersion-managed solitons in a near-zero anomalous-dispersion Er-doped mode-locked fiber laser. Transmissive dual channels are provided by birefringence filtering effect. The dual-wavelength mode-locking centers at 1539.1 and 1578.8 nm with the repetition-rate difference of 420 Hz. Furthermore, 2-hour spectral stability is measured in an open environment, and we analyze the intra-cavity dynamics that influences the long-term stability of the dual-wavelength mode-locked laser operating in the free-running state.

1. Introduction

High measurement accuracy, fast update rate, and large dynamic range make the dual-comb source receive close attention, and it has extensive applications in optical fiber sensing, absolute distance measurement, and molecular spectroscopy (Shao et al., 2016; Coddington et al., 2009; Coddington et al., 2016). Among the multitudinous dual-comb technologies, asynchronous mode-locked pulses generated in fiber lasers with the inherent asynchronous optical sampling (ASOPS) process are considered as a premium option. Unlike two independent mode-locked lasers with slightly different repetition rates, which require complex phase-locked loop (Ycas et al., 2018; Okubo et al., 2015; Casinero et al., 2014), asynchronous pulse sequences generated in a single fiber laser have inherent mutual coherence without additional phase-locking (Hu et al., 2021; Liao et al., 2018; Mehrovar et al., 2016), which is propitious for cost control and miniaturization.

Optional approaches for the generation of asynchronous pulse sequences in a single cavity are bidirectional mode-locking (Saito et al., 2019; Li et al., 2020; Nakajima et al., 2021), orthogonally polarized mode-locking (Akosman and Sander, 2017), and dual-wavelength mode-locking (Hu et al., 2017; Zhao et al., 2011). Single-cavity dual-wavelength mode-locked pulses generally require inter-cavity hump-shaped filters, such as birefringence filters (Hu et al., 2017); Sagnac loop filters

(Li et al., 2018), and fiber Bragg gratings (He et al., 2009), to suppress gain competition. Additionally, the tunable attenuator can also be used to change the intra-cavity loss to achieve equivalent filtering (Zhao et al., 2011). Among these filtering mechanisms, birefringence filter has the advantage that the spectral filtering spacing can be adjustable by altering intra-cavity birefringence. In recent few years, with the maturity of intelligent polarization-state control technology, the mode-locked structure of nonlinear polarization evolution (NPE) has a strong appeal (Pu et al., 2019; Pu et al., 2020; Woodward and Kelleher, 2017; Winters et al., 2017; Andral et al., 2015; Genty et al., 2021; Kutz and Brunton, 2015; Girardot et al., 2020). NPE based fiber lasers will challenge the dominance of material saturable absorbers in the commercial field (Kang et al., 2018; Cui and Liu, 2019). Simultaneously, the natural combination of birefringence filter and NPE technology will fill the blank of automatic mode-locking technology of dual-comb sources.

Furthermore, it is a complex dynamic process that pulses with different repetition rates generated from the oscillator collide periodically, and the periodic collisions of dual-wavelength soliton mode-locking have been observed by Time-stretch dispersive Fourier transform (TS-DFT) (Wei et al., 2018; Wang et al., 2020; Liu et al., 2020; Cui et al., 2021). However, the annihilation and reconstruction of the Kelly sidebands during the collisions are detrimental to the long-term operation of fiber lasers (Wei et al., 2018). Dispersion-managed solitons

^{*} Corresponding authors.

E-mail addresses: yjsong@tju.edu.cn, huminglie@tju.edu.cn (M. Hu).

¹ The two authors contribute equally to this work.

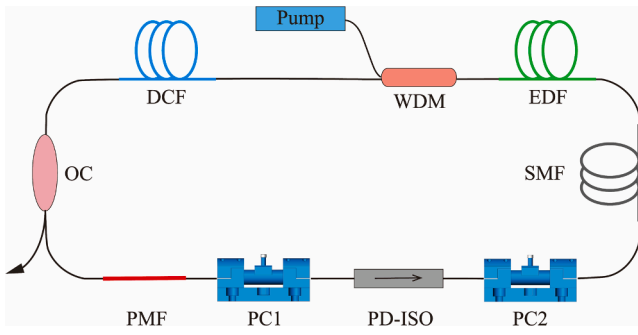


Fig. 1. Schematic of dual-wavelength dispersion-managed soliton mode-locked fiber laser with birefringence-filtered NPE technology.

without Kelly sidebands operating in the near-zero dispersion regime may perform better and have lower quantum noise (Zou et al., 2020; Zou et al., 2021). To date, the researches on the dynamics of dual-wavelength mode-locking in the near-zero dispersion regime are still incomplete.

In this paper, we demonstrate dual-wavelength dispersion-managed soliton mode-locking with wide spectral bandwidth in a near-zero anomalous-dispersion all-fiber laser based on birefringence-filtered NPE. Birefringence filtering enables the laser to operate in a switchable single-wavelength mode-locked state. Subsequently, dual-wavelength mode-locked pulses are generated with the appropriate polarization controller orientations. 2-hour spectral stability of free-running dual-wavelength mode-locking state is also measured to analyze the intra-cavity dynamics.

2. Experimental setup

Fig. 1 shows the schematic of the dual-wavelength dispersion-

managed mode-locked fiber laser experimental setup. A 51-cm Er-doped fiber (EDF, LIEKKI Er110-4/125), is backward-pumped by a 976 nm laser diode via a 980/1550 nm wavelength division multiplexer (WDM). The group-velocity dispersion (GVD) of the EDF is $+0.012 \text{ ps}^2/\text{m}$, and the pigtailed of WDM is a 85-cm OFS980 fiber with the GVD of $+0.005 \text{ ps}^2/\text{m}$. The sandwich structure of two polarization controllers (PCs) and a polarization-dependent isolator (PD-ISO) is employed as an artificial saturable absorber based on NPE. PD-ISO plays the dual role of polarizing and maintaining the unidirectional operation of the laser. The birefringence required for dual wavelength mode locking is provided by inserting a 14-cm polarization maintaining fiber (PMF) in front of the sandwich to suppress gain competition. The corresponding spectral filtering bandwidth is 39.6 nm. A 2.1-m dispersion compensation fiber (DCF, Thorlabs DCF38) with the GVD of $+0.048 \text{ ps}^2/\text{m}$ is used to compensate the intra-cavity dispersion to near-zero, and the measured insertion loss of the DCF is about 0.894 dB. The remanent $\sim 6.57 \text{ m}$ fibers including the pigtailed of the components are single-mode fibers (SMFs) with the GVD of $-0.022 \text{ ps}^2/\text{m}$. The overall fiber length of the ring cavity is 10.17 m, and the corresponding estimated dispersion is -0.036 ps^2 , which illustrates that the laser operates at near-zero dispersion. 10 % laser power is output through a 10:90 output coupler (OC) from the ring cavity. The laser spectra are measured by an optical spectrum analyzer (OSA, Yokogawa AQ6370B) with the resolution of 0.02 nm. The pulse sequences and electrical spectra are respectively monitored by a digital oscilloscope (OSC, Tektronix TDS 3052C) and a radio frequency (RF) analyzer (FSA, RIGOL RSA3030) through a 1.2 GHz photodetector (PD, Thorlabs DET01CFC). The actual pulse width is measured by an autocorrelator (APE Pulse Check).

3. Experimental results and discussion

Initially, with the appropriate intra-cavity PC orientations, the laser can operate in continuous wave (CW) lasing, single-wavelength mode-locking, and dual-wavelength mode-locking regimes at the pump power

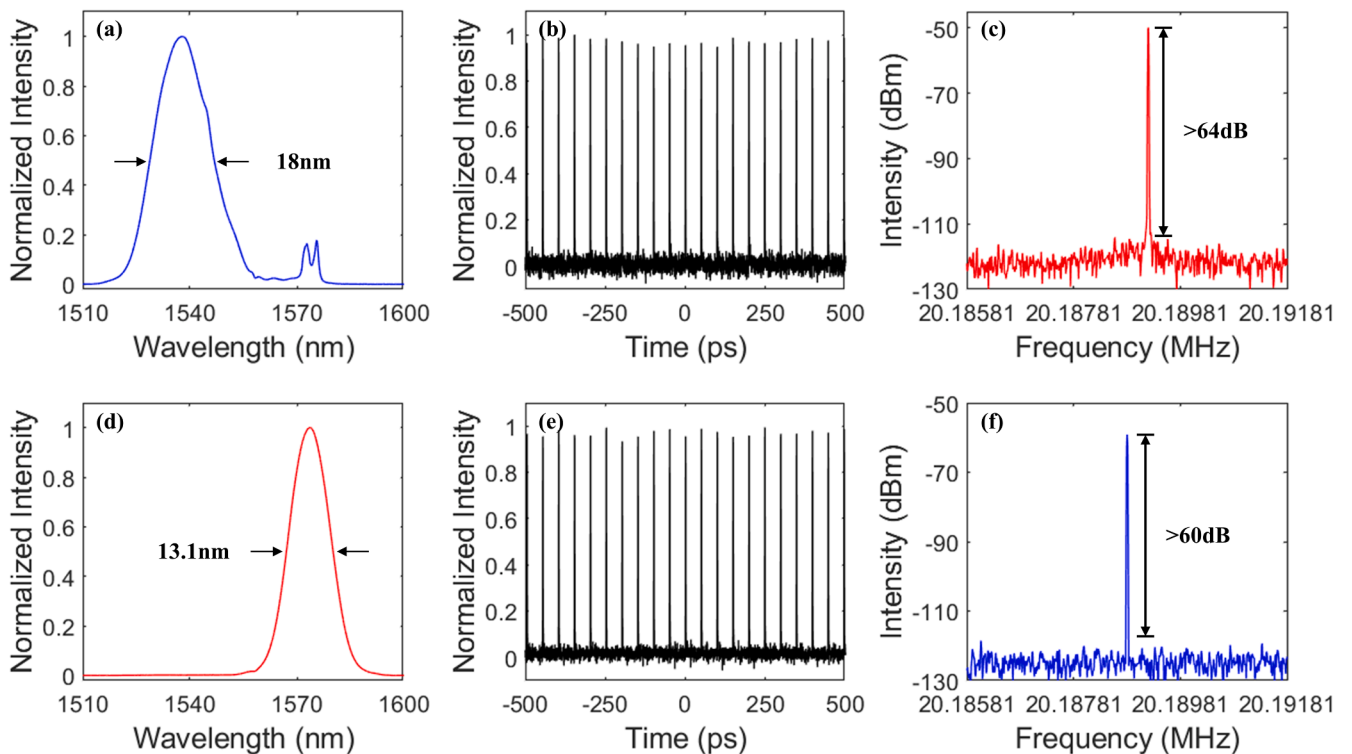


Fig. 2. Switchable single-wavelength dispersion-managed soliton mode-locking. (a) and (d) The optical spectra of 1537.8 nm and 1573.6 nm mode-locking. (b) and (e) The temporal pulse sequences with the round-trip time of $\sim 49.6 \text{ ns}$. (c) and (f) The repetition rates are 20.189213 MHz and 20.188813 MHz, respectively, with the RBW of 30 Hz.

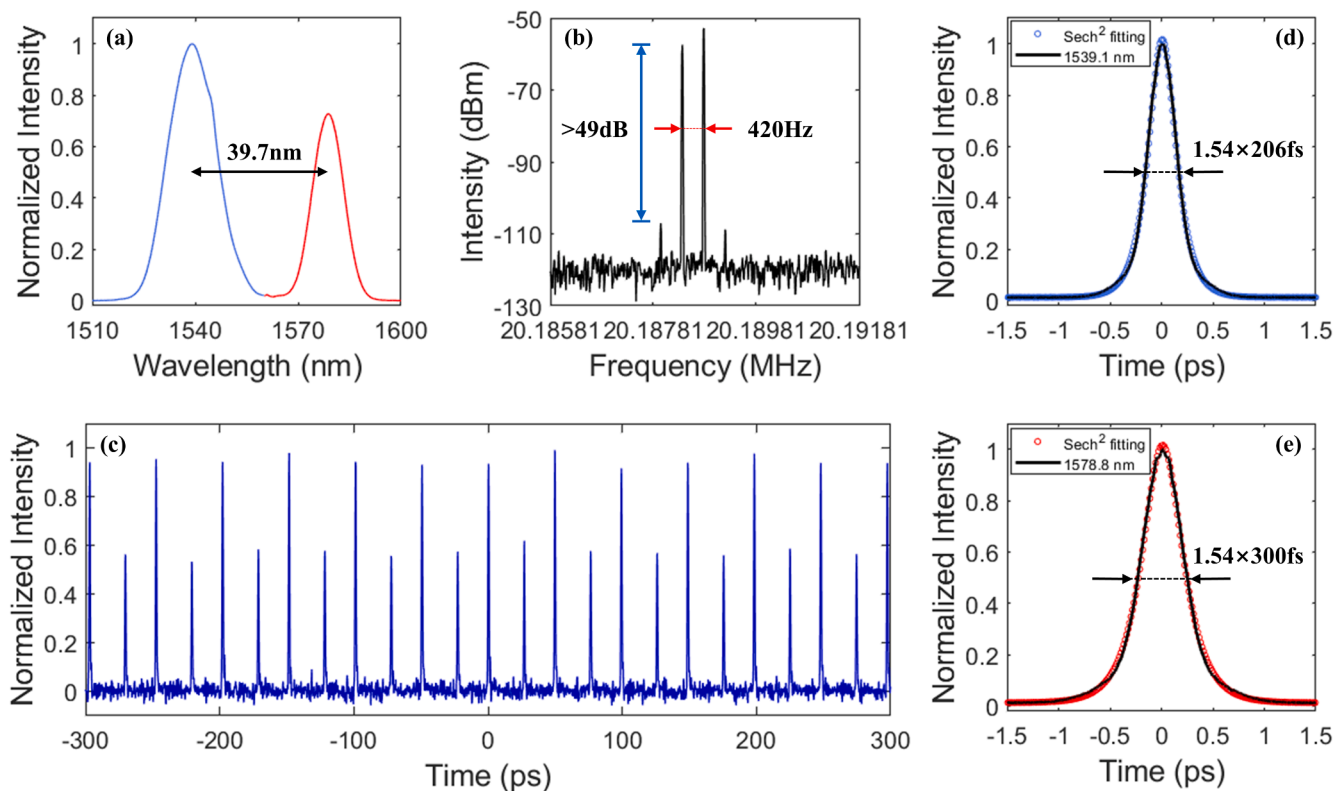


Fig. 3. Dual-wavelength dispersion-managed soliton mode-locking. (a) The optical spectrum with the center wavelength of 1539.1 and 1578.8 nm. (b) The RF spectrum with the RBW of 30 Hz. (c) The temporal waveform containing two pulse sequences. (d) and (e) The optical autocorrelation traces of short- and long-wavelength mode-locking, respectively.

of 106.6 mW. The switchable single-wavelength mode-locking is depicted in Fig. 2. Periodic stretch and compression of pulses circulation in the oscillator suppresses the formation of Kelly sidebands, as shown in Fig. 2(a) and (d). The spectral full width at half maximum (FWHM) of the single-wavelength mode-locking at 1537.8 nm is 18 nm, and at 1573.6 nm is 13.1 nm. The generation of small bumps around 1570 nm, as shown in Fig. 2(a), originates from the gain competition slightly suppressed by birefringent filtering effect, and the intensity of the bumps gradually increases with deeper modulation depth of filter by cautiously adjusting the PCs (Zhu et al., 2019). Slight fluctuations near the spike in the RF spectrum reflect small bumps in the optical spectrum. However, the signal-to-noise ratio (SNR) is still beyond 64 dB, proving the stable operation of the laser, as shown in Fig. 2(c). Differently, the spectrum in Fig. 2(d) illustrates that the short-wavelength frequency component of long-wavelength mode-locking is almost completely suppressed, indicating stronger gain competition. The corresponding RF spectrum in Fig. 2(f) has a relatively flat noise floor, and the SNR is over 60 dB with the resolution bandwidth (RBW) of 30 Hz.

The birefringence filtering position and modulation depth can be changed by rotating the PC orientations. The transmission test of Lyot-filter in Ref. (Zhu et al., 2019) intuitively reflects the spectral response of the birefringence filtering. Without altering the pump power, appropriately adjusting the PCs, dual-wavelength mode-locking can be observed, as shown in Fig. 3. The optical spectrum depicted in Fig. 3(a) exhibits two spectral humps centered at 1539.1 and 1578.8 nm, which exactly match the two adjacent channels of birefringence filter. The corresponding FWHMs are 16.4 nm and 10.6 nm, respectively. Lower intensity and narrower bandwidth of 1578.8 nm mode-locking are caused by weak gain competition and lower gain distribution at long-wavelength. Fig. 3(b) depicts the RF spectrum that two main peaks are located at 20.188373 MHz and 20.188793 MHz, corresponding to the repetition rates of the pulse sequences centered at 1578.8 nm and 1539.1 nm, respectively. The two main RF spectral peaks have a

frequency difference of ~ 420 Hz, which is caused by different group velocities between the asynchronous pulses. The SNR is over 49 dB with the RBW of 30 Hz. The two weak sidebands are attributed to the beat of the two combs generated from the PD, proving the inherent mutual coherence of the dual-comb source (Luo et al., 2019). The OSC captures a moment of the temporal waveform, as shown in Fig. 3(c). The temporal waveform consists of two asynchronous pulse sequences. Pulses with different group velocities chase each other in the oscillator and collide every 2.38 ms (corresponding to 420 Hz repetition-rate difference), which is known as ASOPS (Zhao et al., 2016; Shi et al., 2018). The autocorrelation traces of the pulses centered at 1539.1 and 1578.8 nm is measured separately by a coarse wavelength division multiplexer (CWDM) which transmits the laser with wavelengths less than 1560 nm while reflecting the remaining frequency components of the laser. The autocorrelation traces of short- and long-wavelength pulses are shown in Fig. 3(d) and (e). The pulse FWHMs are 206 fs and 300 fs, respectively, with the assumption of Sech² shape. The time-bandwidth products (TBPs) for the 1539.1 and 1578.8 nm pulses are 0.427 and 0.383, respectively, which are slightly larger than the Fourier-transform limit of 0.315, indicating that the pulses are slightly chirped. Even though there is no Kelly sideband in the spectrum, the autocorrelation trace can be well fitted by the Sech² shape and the TBP is close to the transform limit, indicating that the laser still operates in the soliton state.

Single-cavity dual-comb sources, which can generate two sets of mode-locked pulse sequences with a certain repetition frequency difference, are considered as a possible candidate for the current bulky and complex dual-comb systems. Different from single-wavelength mode-locked lasers, the intra-cavity dynamics of asynchronous pulses sharing the same optical oscillator is more complicated, which has attracted the attention of many researchers. However, relevant researches have mainly focused on the transient dynamics of collision and initiation of dual-wavelength mode-locked pulses, so far.

The dynamic process under long-term operation is equally important

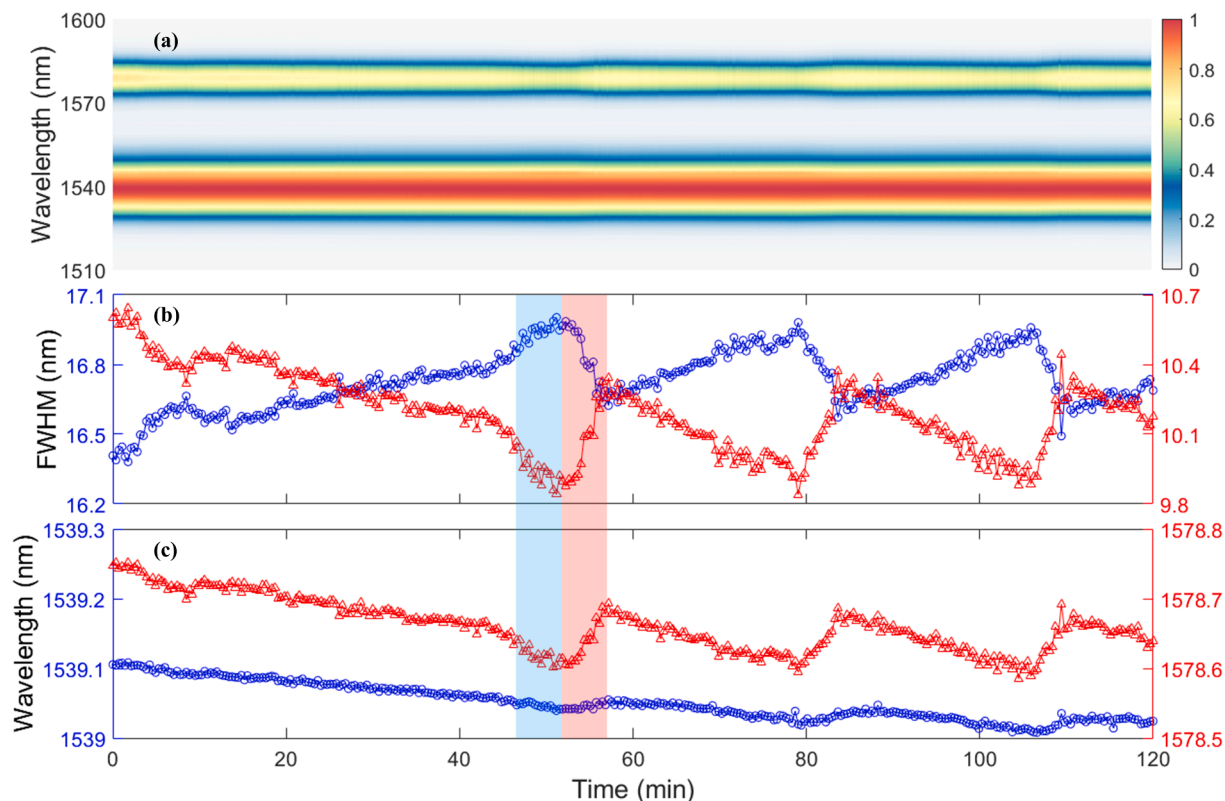


Fig. 4. 2-hour spectral stability test of the dual-wavelength mode-locked laser. (a) Evolution of the optical spectra in 2 h. (b) Spectral FWHM variations of mode-locking centered at 1539.1 (blue circles) and 1578.8 nm (red triangles). (c) Center wavelength variations of mode-locking centered at 1539.1 (blue circles) and 1578.8 nm (red triangles). (For interpretation of the references to colour in this figure legend, the reader is referred to the web version of this article.)

for the applications of dual-comb sources. Therefore, the 2-hour spectral stability of the free-running dual-wavelength mode-locked laser is measured without external active vibration isolation and temperature control, as shown in Fig. 4. The output spectral evolution of dual-wavelength mode-locked laser is measured at a spectral update rate of 0.25 Hz. The variation of spectral FWHMs and center wavelengths are extracted separately for a clearer and more intuitive analysis of long-term dynamics of the dual-wavelength mode-locked laser, as shown in Fig. 4(b) and (c). The spectral FWHM variation can be considered as an observing evidence of gain competition. The gain sometimes flows to the long-wavelength and sometimes to the short-wavelength, so the dual-wavelength mode-locked state can be seen as the dynamic balance of gain competition. We found that “breathing” processes in the colored area of Fig. 4 (b) have a large “breathing” ratio, which may originate from the fact that coherent frequency components (known from the two sub-peaks in Fig. 3(b)) facilitate the flow of gain. The variation of center wavelengths is shown in Fig. 4(c). The shift of the central wavelengths to shorter wavelength is mainly attributed to the temperature drift which induces subtle shifts of the dual-wavelength mode-locked state and the position of filtering channels. However, the wavelengths have obvious fluctuations in the colored area. Initially, in the blue area, the wavelengths shift to shorter wavelength influenced by temperature drift, however the slope gradually approaches zero. Limited by the gain distribution, the short-wavelength mode-locked FWHM does not continue to broaden. In the red area, as the wavelength continues to blue-shift, the narrowed FWHM instead shifts the center wavelength toward long wavelength, which is exactly opposite for the case of the long-wavelength mode-locking.

The mutual coupling of environmental disturbances, birefringence filtering effect and limited gain distribution results in the “breathing” processes and fluctuations of wavelengths. With external active temperature control, increasing the filter spacing or narrowing the spectral

bandwidth can slow down the “breathing” and improve the long-term stability of the dual-wavelength mode-locked laser.

4. Conclusion

Switchable single-wavelength soliton and dual-wavelength soliton are generated in a dispersion-managed Er-doped mode-locked fiber laser by the birefringence-filtering effect and NPE technology. By adjusting the PCs to introduce a linear phase shift, the filtering position is shifted so that the wavelength of mode-locking can be switched. When the gain distribution is matched with birefringence filtering channels, the laser operates in a dual-wavelength mode-locked state. The suppression of the Kelly sidebands makes the optical spectrum wider, however the auto-correlation traces of the asynchronous pulses can be well fitted by sech^2 shape, indicating that the laser still operates in the soliton regime. We monitor the spectral stability for 2-h using the OSA and extract the characteristic information from the spectral evolution to explore the intra-cavity dynamics. Spectral coherent frequency components of mode-locking at different wavelengths affect the “breathing” ratio of the spectral FWHMs. On the other hand, due to the limited gain distribution, the mode-locked wavelength shifts caused by temperature drift fluctuate, which does not occur in the case of active temperature control.

Declaration of Competing Interest

The authors declare that they have no known competing financial interests or personal relationships that could have appeared to influence the work reported in this paper.

Acknowledgements

This work was supported by the Project of Guangdong Province,

China (2018B090944001) and the National Natural Science Foundation of China (61827821, 61975144).

References

- Akosman, A.E., Sander, M.Y., 2017. Dual comb generation from a mode-locked fiber laser with orthogonally polarized interlaced pulses. *Opt. Express* 25 (16), 18592–18602. <https://doi.org/10.1364/OE.25.018592>.
- Andral, U., Fodil, R.S., Amrani, F., Billard, F., Hertz, E., Grelu, P.J.O., 2015. Fiber laser mode locked through an evolutionary algorithm. *Optica* 2 (4), 275–278. <https://doi.org/10.1364/OPTICA.2.000275>.
- Cassinero, M., Gambetta, A., Coluccelli, N., Laporta, P., Galzerano, G.J.A.P.L., 2014. Absolute dual-comb spectroscopy at 1.55 μm by free-running Er: fiber lasers. *Appl. Phys. Lett.* 104 (23), 231102 <https://doi.org/10.1063/1.4882862>.
- Coddington, I., Swann, W.C., Nenadovic, L., Newbury, N.R., 2009. Rapid and precise absolute distance measurements at long range. *Nat. Photonics* 3 (6), 351–356. <https://doi.org/10.1038/nphoton.2009.94>.
- Coddington, I., Newbury, N., Swann, W., 2016. Dual-comb spectroscopy. *Optica* 3 (4), 414–426. <https://doi.org/10.1364/OPTICA.3.000414>.
- Cui, Y., Liu, X., 2019. Revelation of the birth and extinction dynamics of solitons in SWNT-mode-locked fiber lasers. *Photon. Res.* 7 (4), 423–430. <https://doi.org/10.1364/PRJ.7.000423>.
- Cui, Y., Zhang, Y., Song, Y., Huang, L., Tong, L., Qiu, J., Liu, X., 2021. XPM-induced vector asymmetrical soliton with spectral period doubling in mode-locked fiber laser. *Laser Photonics Rev.* <https://doi.org/10.1002/lpor.202000216>, 152000216.
- Genty, G., Salmela, L., Dudley, J.M., Brunner, D., Kokhanovskiy, A., Kobtsev, S., Turitsyn, S.K.J.N.P., 2021. Machine learning and applications in ultrafast photonics. *Nat. Photonics* 15 (2), 91–101. <https://doi.org/10.1038/s41566-020-00716-4>.
- Girardot, J., Billard, F., Coillet, A., Hertz, E., Grelu, P., 2020. Autosetting mode-locked laser using an evolutionary algorithm and time-stretch spectral characterization. *IEEE J. Sel. Top. Quantum Electron.* 26 (5), 1–8. <https://doi.org/10.1109/JSTQE.2020.2985297>.
- He, X., Fang, X., Liao, C., Wang, D.N., Sun, J., 2009. A tunable and switchable single-longitudinal-mode dual-wavelength fiber laser with a simple linear cavity. *Opt. Express* 17 (24), 21773–21781. <https://doi.org/10.1364/OE.17.021773>.
- Hu, G., Pan, Y., Zhao, X., Yin, S., Zhang, M., Zheng, Z., 2017. Asynchronous and synchronous dual-wavelength pulse generation in a passively mode-locked fiber laser with a mode-locker. *Opt. Lett.* 42 (23), 4942–4945. <https://doi.org/10.1364/OL.42.004942>.
- Hu, D., Wu, Z., Cao, H., Shi, Y., Li, R., Tian, H., Song, Y., Hu, M., 2021. Dual-comb absolute distance measurement of non-cooperative targets with a single free-running mode-locked fiber laser. *Opt. Commun.* 482 <https://doi.org/10.1016/j.optcom.2020.126566>.
- Kang, Z., Liu, M., Tang, C., Xu, X., Jia, Z., Qin, G., Qin, W., 2018. Microfiber coated with gold nanorods as saturable absorbers for 2 μm femtosecond fiber lasers. *Optical Mater. Express* 83841. <https://doi.org/10.1364/OME.8.003841>.
- Kutz, J.N., Brunton, S.L.J.N., 2015. Intelligent systems for stabilizing mode-locked lasers and frequency combs: machine learning and equation-free control paradigms for self-tuning optics. *Nanophotonics* 4 (4), 459–471. <https://doi.org/10.1515/nanoph-2015-0024>.
- Li, R., Shi, H., Tian, H., Li, Y., Liu, B., Song, Y., Hu, M., 2018. All-polarization-maintaining dual-wavelength mode-locked fiber laser based on Sagnac loop filter. *Opt. Express* 26 (22), 28302–28311. <https://doi.org/10.1364/OE.26.028302>.
- Li, B., Xing, J., Kwon, D., Xie, Y., Prakash, N., Kim, J., Huang, S.-W., 2020. Bidirectional mode-locked all-normal dispersion fiber laser. *Optica* 7 (8). <https://doi.org/10.1364/optica.396304>.
- Liao, R., Song, Y., Liu, W., Shi, H., Chai, L., Hu, M., 2018. Dual-comb spectroscopy with a single free-running thulium-doped fiber laser. *Opt. Express* 26 (8), 11046–11054. <https://doi.org/10.1364/OE.26.011046>.
- Liu, M., Li, T.-J., Luo, A.-P., Xu, W.-C., Luo, Z.-C., 2020. “Periodic” soliton explosions in a dual-wavelength mode-locked Yb-doped fiber laser. *Photon. Res.* 8 (3) <https://doi.org/10.1364/prj.377966>.
- Luo, X., Tuan, T.H., Saini, T.S., Nguyen, H.P.T., Suzuki, T., Ohishi, Y., 2019. Tunable and switchable all-fiber dual-wavelength mode locked laser based on Lyot filtering effect. *Opt. Express* 27 (10), 14635–14647. <https://doi.org/10.1364/OE.27.014635>.
- Mehravar, S., Norwood, R.A., Peyghambarian, N., Kieu, K.J.A.P.L., 2016. Real-time dual-comb spectroscopy with a free-running bidirectionally mode-locked fiber laser. *Appl. Phys. Lett.* 108 (23), 231104 <https://doi.org/10.1063/1.4953400>.
- Nakajima, Y., Kusumi, Y., Minoshima, K., 2021. Mechanical sharing dual-comb fiber laser based on an all-polarization-maintaining cavity configuration. *Opt. Lett.* 46 (21), 5401–5404. <https://doi.org/10.1364/OL.440818>.
- Okubo, S., Iwakuni, K., Inaba, H., Hosaka, K., Onae, A., Sasada, H., Hong, F.-L., 2015. Ultra-broadband dual-comb spectroscopy across 1.0–1.9 μm . *Appl. Phys. Express* 8 (8), 082402. <https://doi.org/10.7567/apex.8.082402>.
- Pu, G., Yi, L., Zhang, L., Hu, W.J.O., 2019. Intelligent programmable mode-locked fiber laser with a human-like algorithm. *Optica* 6 (3), 362–369. <https://doi.org/10.1364/OPTICA.6.000362>.
- Pu, G., Yi, L., Zhang, L., Luo, C., Li, Z., Hu, W.J.L.S., 2020. Intelligent control of mode-locked femtosecond pulses by time-stretch-assisted real-time spectral analysis. *Light Sci. Appl.* 9 (1), 1–8. <https://doi.org/10.1038/s41377-020-0251-x>.
- Saito, S., Yamanaka, M., Sakakibara, Y., Omoda, E., Kataura, H., Nishizawa, N., 2019. All-polarization-maintaining Er-doped dual comb fiber laser using single-wall carbon nanotubes. *Opt. Express* 27 (13), 17868–17875. <https://doi.org/10.1364/OE.27.017868>.
- Shao, L.-Y., Liang, J., Zhang, X., Zou, X., Luo, B., Pan, W., Lianshan, Y., 2016. High resolution refractive index sensing with dual-wavelength fiber laser. *IEEE Sens. J.* 1–1 <https://doi.org/10.1109/jSEN.2016.2616487>.
- Shi, H., Song, Y., Li, T., Wang, C., Zhao, X., Zheng, Z., Minglie, H., 2018. Timing jitter of the dual-comb mode-locked laser: a quantum origin and the ultimate effect on high speed time/frequency domain metrology. *IEEE J. Sel. Top. Quantum Electron.* PP1-1 <https://doi.org/10.1109/JSTQE.2018.2810381>.
- Wang, X., He, J., Shi, H., Mao, B., Feng, M., Wang, Z., Yue, Y., Liu, Y.-G., 2020. Real-time observation of multi-soliton asynchronous pulsations in an L-band dissipative soliton fiber laser. *Opt. Lett.* 45 (17), 4782–4785. <https://doi.org/10.1364/OL.400409>.
- Wei, Y., Li, B., Wei, X., Yu, Y., Wong, K.K.Y., 2018. Ultrafast spectral dynamics of dual-color-soliton intracavity collision in a mode-locked fiber laser. *Appl. Phys. Lett.* 112 (8) <https://doi.org/10.1063/1.5020821>.
- Winters, D.G., Kirchner, M.S., Backus, S.J., Kapteyn, H.C., 2017. Electronic initiation and optimization of nonlinear polarization evolution mode-locking in a fiber laser. *Opt. Express* 25 (26), 33216–33225. <https://doi.org/10.1364/OE.25.033216>.
- Woodward, R., Kelleher, E.J.O.L., 2017. Genetic algorithm-based control of birefringent filtering for self-tuning, self-pulsing fiber lasers. *Opt. Lett.* 42 (15), 2952–2955. <https://doi.org/10.1364/OL.42.002952>.
- Ycas, G., Giorgetta, F.R., Baumann, E., Coddington, I., Herman, D., Diddams, S.A., Newbury, N.R., 2018. High-coherence mid-infrared dual-comb spectroscopy spanning 2.6 to 5.2 μm . *Nat. Photonics* 12 (4), 202–208. <https://doi.org/10.1038/s41566-018-0114-7>.
- Zhao, X., Zheng, Z., Liu, L., Liu, Y., Jiang, Y., Yang, X., Zhu, J., 2011. Switchable, dual-wavelength passively mode-locked ultrafast fiber laser based on a single-wall carbon nanotube modelocker and intracavity loss tuning. *Opt. Express* 19 (2), 1168–1173. <https://doi.org/10.1364/OE.19.001168>.
- Zhao, X., Hu, G., Zhao, B., Li, C., Pan, Y., Liu, Y., Yasui, T., Zheng, Z., 2016. Picometer-resolution dual-comb spectroscopy with a free-running fiber laser. *Opt. Express* 24 (19), 21833–21845. <https://doi.org/10.1364/OE.24.021833>.
- Zhu, Y., Xiang, F., Jin, L., Set, S.Y., Yamashita, S., 2019. All-fiber dual-wavelength mode-locked laser using a bend-induced-birefringence lyot-filter as gain-tilt equalizer. *IEEE Photon. J.* 11 (6), 1–7. <https://doi.org/10.1109/jphot.2019.2946380>.
- Zou, D., Zhang, Y., Song, Y., Hu, M., 2020. Sub-100 fs Bound State Solitons and Period-Doubling Bifurcations in a Mode-Locked Fiber Laser. *IEEE Photon. Technol. Lett.* 32 (20), 1311–1314. <https://doi.org/10.1109/LPT.2020.3021486>.
- Zou, D., Li, Z., Qin, P., Song, Y., Minglie, H., 2021. Quantum limited timing jitter of soliton molecules in a mode-locked fiber laser. *Opt. Express* 29. <https://doi.org/10.1364/OE.437553>.